0

Photoluminescence

Introduction:

Photoluminescence spectroscopy is a useful technique for characterization and study of materials. It is most widely used technique for characterizing III-V semiconductors and their alloys. It is a simple and elegant technique that provides wealth of information with minimum waste of time. It is used for the study of recombination processes as well as for the quality determination.

PL is used to study the bulk or the epitaxial films for their inter and intra wafer variation and to compare material grown by different techniques. The information thus obtained becomes important when the material is to be used for optoelectronic devices.

However it does not give an all-encompassing view of every aspect of the optical properties of the materials, which makes it necessary to rely upon complementary information.

What is Photoluminescence spectroscopy?

It relies on the creation of electron-hole pairs by incident radiation and subsequent radiative recombination with photon emission. Measuring of the energy distribution of emitted photons after optical excitation follows this.

In an emission process an electron (or a quasi-particle) occupying a higher energy state makes a quantized (i.e. discrete) transition to an

empty lower energy state. For a radiative transition the energy difference between the two is emitted as electromagnetic radiation i.e. photons whereas for non-radiative transitions the energy difference is emitted in the form of heat i.e. phonons. The recombination is a non-equilibrium process since energy must be conserved.

For radiative transitions the Fermi's golden rule states that the product of empty states in lower energy levels and the density of carriers in the higher energy levels determine the radiation rate. The rate is expressed as the number of photons generated per unit time. Secondly the spectrum (energy distribution of photons) is much narrower than that due to absorption. This is because emission processes occur between a narrow band of states occupied by thermalized electrons with a narrow band of empty states at the top of valence band.

Applications and limitations:

PL is useful in quantifying:

1. Optical emission efficiencies
2. Composition of material i.e. alloy composition
3. Impurity content
4. Layer thickness i.e. Quantum well thickness

Limitations:

1. It does not give any information regarding the temporal kinetics, transport dynamics, or the spatial distribution of the light emission. These factors become important since semiconductor devices deal with high-speed devices, nanostructured and transport devices.
2. The determination of concentration of impurity is difficult.

In order to demonstrate PL for assessing properties and for studying properties of semiconductor physics relevant to recombination processes. We have to review the band structure, free carrier

properties, quasi and many particle states, impurities and recombination processes and properties related to nanostructure as these are related to the emission processes.

Absorption and photoluminescence emission

Semiconductors interact with electromagnetic waves. The dominant effect is absorption at the energy gap and under certain conditions this leads to photoluminescence. A photon whose energy is equal or exceeds the energy gap can excite a valence electron into a higher energy state. The absorption coefficient is proportional to the density of states in the initial and final states and to the probability that one transition takes place. Energy is conserved and because of the fact that momentum of light is 10^3 times smaller than the momentum of the electrons, the wave

vector **k** is nearly conserved, too. In this case we speak about direct transitions but there are very few semiconductors that have a direct gap (GaAs), so that there is a need for a third body to realize indirect transitions. The third body interaction with a phonon makes indirect absorption far less probable than direct absorption and therefore the absorption is weaker. After the absorption process separating electrons and positively charged holes both particles recombine. The rate of recombination depends thereby again on the density of states and probability for the recombination.

In many ways photoluminescence is the inverse process of absorption. But when we compare the calculation for the recombination and absorption coefficient, we see that an absorption experiment shows a threshold for the gap but photoluminescence shows a sharp peak.

Absorption coefficient (α) is given by:

$$\alpha = C \sum n_i n_f R_f ,$$

where n_i, n_f are the density of initial and final states respectively, R_f is the transition probability, C is a constant. Summation over all states separated by the photon energy gives:

$$\alpha = A(\hbar\omega - E_{gap})^p ,$$

where p = 1/2 or 3/2 (quantum rules).

Generally absorption experiments give more information about the energetic structure of the sample and with them one can better determine the energy gap even if the sample has impurity levels. The existence of excitons makes absorption examinations particularly interesting. An absorption measurement determines the gap between the top of the valence band and the Fermi level. We can see energy states around the fundamental gap even at low temperatures (Boltzmann Distribution) but the disadvantage is that we have to prepare a very thin sample.

In conventional photoluminescence the photon comes from all the transitions between the bottom of the conduction band and the Fermi level to the top of the valence band.

A tool combining the effects of absorption and photoluminescence excitation spectroscopy (PLE). The laser providing a fixed wavelength is replaced by a tunable dye laser or less expensively by a spectrometer and a powerful white lamp (Dawson 1983) and the analyzing spectrometer is set at a fixed wavelength (often the main luminescence). In this way we can measure the absorption of the varied exciting energy.

Types of Recombination

1. Band-to- band
2. Excitonic (free and bound)
3. Free-to-bound transitions

4. Phonon assisted
5. Auger Recombination

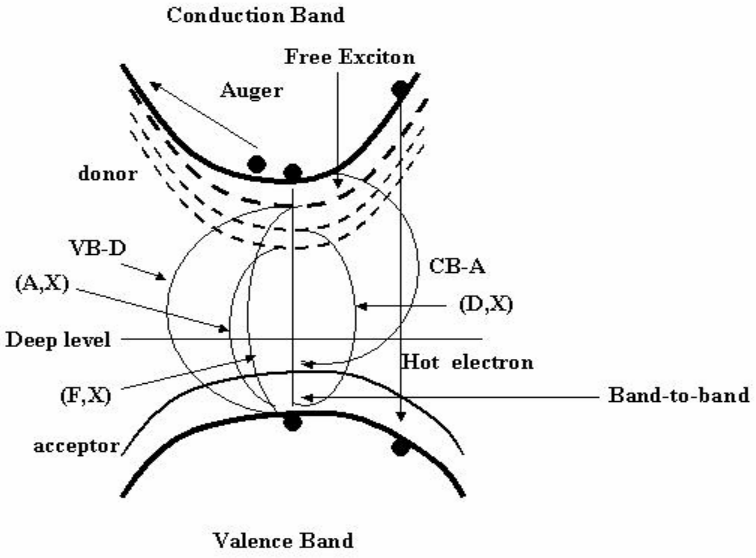

Figure 1 Showing various types of Recombination.

Excitons

The electron hole system coupled through the coloumbic interaction is

termed as exciton. This introduces bound states in between the forbidden energy bandgap. The distance between them is large. This kind of transition is existent at low temperatures and in high purity samples due to low binding energy. In the poorer quality samples the excitonic transitions merge with the band-to-band transitions. These transitions hence are studied mainly from the view of material characterization. With the advent of heterostructures the importance of excitons has increased a lot due to higher binding energies (explained below). The binding energy of the excitons is given by:

$$E_{3D-exciton} = \frac{\mu^* e^4}{32\pi^2 \hbar^2 e^2 e_0{}^2 n^2} + \frac{\hbar^2 k}{2(m_e^* + m_h)}$$

where μ is the reduced effective mass of electrons and holes

$$\frac{1}{\mu} = \frac{1}{m_e^*} + \frac{1}{m_h^*}$$

Where the second term in it is equal to the kinetic energy of the whole exciton described by its wave vector k and can be neglected in most cases. With the use of this equation the binding energy of excitons is equal to 4.2 meV in bulk GaAs (Wannier excitons [9]).

Typically the excitonic binding energy is of the order of 2- 6 meV in most of the semiconductors.

The binding energy for excitons increases in the quantum well structures because of confinement. The higher surrounding potential barriers trap the exciton and this leads to a higher binding energy. The localization is increased and due to the increase of the recombination

rate it is easier to observe the exciton than in the bulk material. For infinite potential barrier we can assume that the binding energy for 2-D exciton is as follows:

$$E_{2Dexciton} = E_{3Dexciton} \frac{n^2}{\left(n - \frac{1}{2}\right)^2}$$

For GaAs we get 16.8 meV, which is rather big. It is difficult to calculate the binding energy of the excitons in 2 – D structures.

We find that both the magnitude and the qualitative behavior of the energy levels of excitons calculated using finite barrier heights are quite different from those obtained from infinite potential barrier heights. This is very well justified in the case when x < .3 where the band discontinuities cannot be treated as infinite(esp. for the valence band where it is only 15% of the total height).

For a given value of x the value of E_{ex} increases first as the L is reduced until it reaches a maximum and then decreases quite rapidly. The value of the maxima depends upon both the value of x and the length of the well. The value of L at which E reaches a maximum is smaller for larger x.

The Wannier excitons [3] exist in ground states as well a excited states like 1*s*, 2*s*, 2*p* etc. The binding energy of the ground and excited state are shown in the graph [Ronald L Greene].

.

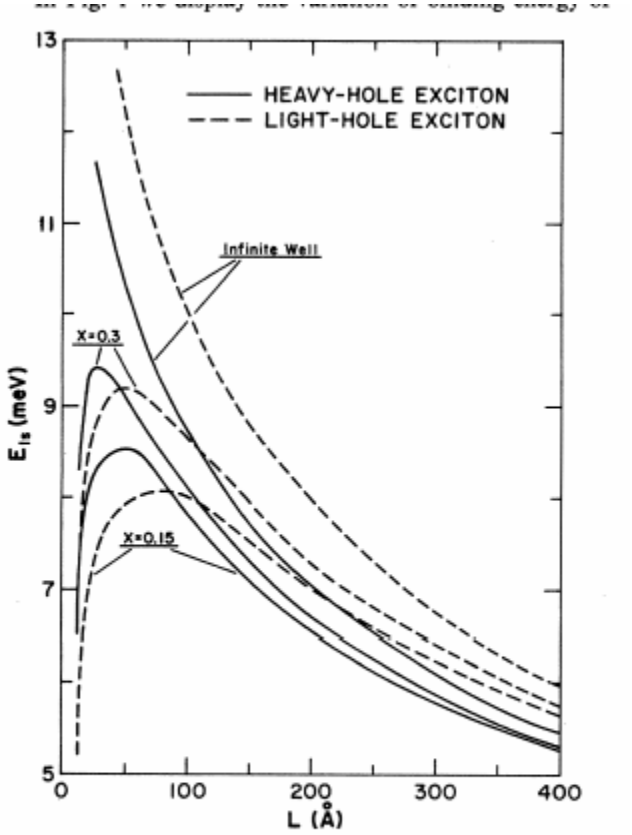

FIG. 1. Variation of the binding energy of the ground state, E_{1s}, of a heavy-hole exciton (solid lines) and a light-hole exciton (dashed lines) as a function of the GaAs quantum-well size (L) for Al concentrations $x=0.15$ and 0.3, and for an infinite potential well.

However, the binding energy in our case is of the order of 6meV (ground state), though that found out from the figure is about 10 meV.The reason behind it is that the samples that we have used are doped and hence the excitonic binding energies in presence of other carriers is reduced the effect is explained below.

Depending on the density of carriers, the excitonic absorption can either depress or fully quenched. The physics behind these is given by the many body effects, which are divided into three different categories. The first comes from the Pauli's exclusion principle. Electrons and the holes, which make up the excitons, are fermions. If an electron occupies a state, the transition of another electron from valence band is forbidden into that state this is known as phase space

filling. The second process is the carrier screening to the electron hole interaction. The screening reduces the coulombic interaction between the two particles and this in turn reduces the excitonic binding energy and the lifetime. The last mechanism is the short-range exchange and the correlation interactions among carriers that play an important role in case of 2D structures [1].

It is important to note that the above mentioned discussions are valid only for a semiconductor with intrinsic carrier concentration.

EXCITONIC OSCILLATOR STRENGTH:

The excitonic strength of 1H-1C exciton as a function of the carrier concentration at low temperatures is given by:

$$\frac{f_{1s}(N)}{f_{1s}(0)} = \frac{1}{1+\frac{N}{N_C}}$$

Where *f* factor denotes the oscillator strength and $N_C = \frac{2}{\pi a_0^{\,2}}$.

The results show that after the critical density N_c the f_{1s} falls off rapidly with carrier concentration.

The N_c is defined as the density at which:

$$f_{1s}(N = N_c) = \frac{1}{2} f_{1s}(N = 0)$$

For our case it comes out to be around $10^{11}/cm^3$.

EXCITONIC BINDING ENERGY: the effect of phase space filling on the excitonic binding energy ncan be found out with the help of Schrodinger equation the result for such calculations give:

$$E_{XB}(N) = E_{XB}(0)\left[1 - \frac{N}{N_C}\right]^2$$

The equation explicitly shows the decline of binding energy with

increase of carriers.

The calculations done for the above equation use the effective dielectric constant as

$$\varepsilon(N) = \frac{\varepsilon(0)}{1 - \frac{N}{2N_C}}$$

The absorption spectra from n-type modulation MQW's with well width of 200 Å and various electron and various electron densities is been reported. The absorption by excitons decreases with increases two dimensional electron gas density. The resonant peaks also broaden with carrier density.

It is not easy to measure directly the change in binding energy of the exciton with varying carrier density. What we can measure is directly the optical transition energy (peak energy) for each excitonic sub bands in MQW's. The energies of those peaks are affected by many factors depending on the QW thickness, the band gap renormalization of the band gap and on the excitonic binding energy. Since the peak energy fluctuations of the QW thickness and that due to BGN are of the same order as that as the excitonic binding energy hence it becomes difficult to obtain BE accurately.

One way of determining it is by using unique properties related to the excitons. There are two important factors that distinguish the phase space filling from other effects;

1. Phase space filling only affects the filled sub bands while BGR and QW thickness affect all the sub bands.
2. it is strongly temperature dependent

Using the above properties we can calculate the excitonic binding

energy change due to phase space filling (PSF) qualitatively. The peak energy can be measured for LH – HH respectively as a function of temperature. And the difference between 1C-1HH and
1C-1LH

$$\Delta E(T) = E_{1C-1L} - E_{1C-1H}$$
$$\Delta E(T) = CONSTANT + \left(\Delta E_{1C-1L}{}^{PSF} - \Delta E_{1C-1H}{}^{PSF}\right)$$

the constant describes the temperature insensitive parts such as confinement energies, the excitonic binding energies and their changes due to screening and other many body effects,etc.the BG temperature dependence is cancelled .the only temperature dependent terms are $\Delta E_{1C-1L}{}^{PSF} and \Delta E_{1C-1H}{}^{PSF}$ .for n – type samples the shift in heavy hole closely follows that of the light hole but in the p-type samples only the first HH sub band is occupied not the LH peak. $\Delta E_{1C-1L}{}^{PSF} = 0$.
The variation of peak energy with carrier concentration if plotted in the figure for -

L_Z = 100 Å

L_B = 100 Å

The samples used there for study are all *modulation doped* structures essentially to study the effect of phase space filling.
The excitonic absorption quenching with phase space filling is shown for n type samples.

The samples that are shown below with Lw = 210, LB= 150, x = .3, ND as shown in the table.

S.No.	N_D (cm^3)	N_S (cm^3)		N_D (cm^3)	N_S (cm^3)
1	**Undoped**		4	**$1x10^{17}$**	**$9.0x10^{10}$**
2	**$3x10^{16}$**	**$2.7x10^{10}$**	**5**	**$3x10^{17}$**	**$2.7x10^{11}$**
3	**$6x10^{16}$**	**$5.4x10^{10}$**	**6**	**$3x10^{18}$**	**$2.7x10^{12}$**

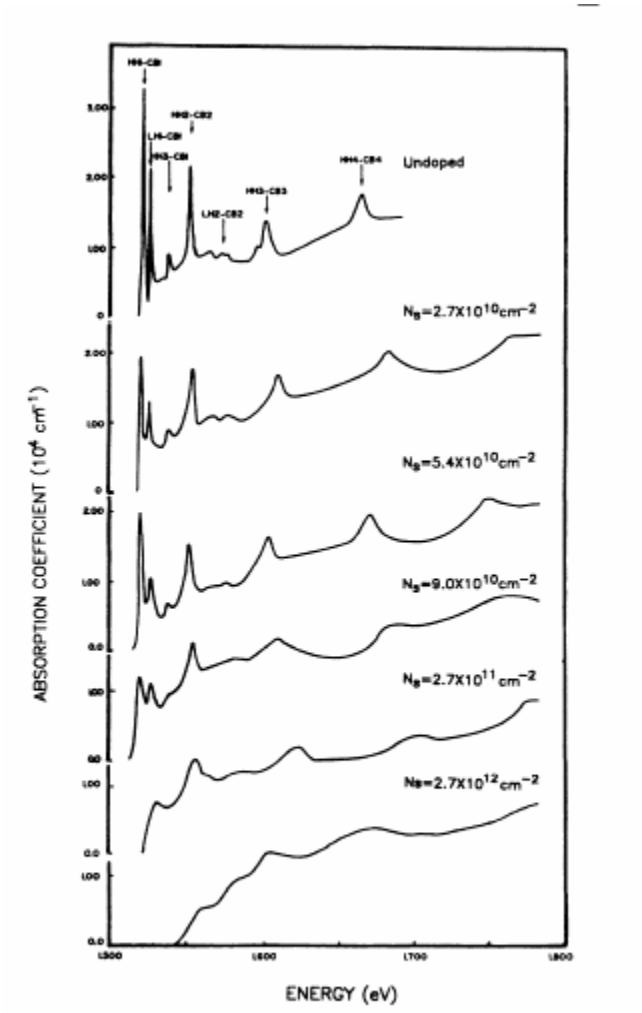

FIG. 3. Absorption spectra for all of the samples with different electron densities as listed in Table I.

It is important to note that when the electronic density goes upto 3×10^{11} cm^{-2} the first heavy hole and light hole peaks merge together (excitonic) and almost totally bleached. Secondly the change in absorption spectra of the lowest sub band is more rapid as compared to that for higher sub bands with increasing electron density. Thirdly, the line shapes for excitonic peaks become broader with increasing density of carriers. And lastly no consistent energy shift for n=1 excitons was observed. The excitonic transitions related to higher

subbands shift to higher energies.

There is a gradual decline in the intensity of the peak and simultaneous broadening of the peak that takes place. Similar results are expected for excitons associated wit other unfilled sub bands.for the excitons in the first subband many body effects become important. a more realistic calculation that takes many body effects by consideration of the single electron hole pair excitations and the shake up process has been made and used to successfully explain the experimentally observed optical emission from electrons confined in GaAs QW with polarization normal to plane. In the calculations of the excitonic oscillations it is found that the system has bound state for Fermi vector k_f less than 0.019Å if the Fermi sea is to be taken into account. The relationship between the k_f and the electron density N is given by $N = (1/2\pi) k_f^2$. For k_f = 0.019 $(Å)^{-1}$ for the corresponding electron density $N = 5.7 \times 10^{11}$ which is in well agreement with experimental value.

The more rapid decline for absorption coefficient of the n = 1 sub band clearly shows that the PSF effects are more pronounced than the other two specified effects i.e. columbic screening and the exchange interactions.

FWHM of a PL spectrum

(relation with excitonic lifetime)

The physical significance of FWHM or the line width is very important to understand. In the case of undoped samples in which no free carriers are present, the line width is determined by the homogenous and the inhomogeneous broadening mechanisms, and is a good measure of the interface quality [14] However in the case of

modulation doped quantum wells the presence of large number of sheet carriers the line width are broadened to a great extent.

At low temperatures the broadening is governed by the extent of localization of the photo excited holes in real space. At low temperatures the photo-excited holes do not have sufficient energy to take part in PL spectra with electrons possessing large k. This typically results in narrow width of the PL spectra contributed by the transitions near **k** = 0. Such behavior is clearly seen in modulation doped QW structures. For electron density in the QW structures the homogenous broadening reflects the lifetime of excitonic oscillations. The presence of the electron gas decreases the excitonic binding energy leading to lesser lifetime. By using the uncertainty principle the lifetime can be approximated as $\tau = \frac{\hbar}{W_{FWHM}}$. In our case the FWHM is being plotted as a function of temperature. the interpretation is given later.

Some studies [14] also show that the broadening of the excitonic peak is also related to the Fermi level (for changes in level of doping) and the fact that the electrons with higher energy in the sub band are available to recombine with partially localized holes making the peak wider with increasing free carriers concentration.

For a particular subband – subband transition the width of the PL peak can be approximated by the difference between the Fermi level and the first electron level. This difference times the density of states gives the 2D doping as

$$\frac{\delta}{FWHM} = \frac{4\pi m^*}{h^2}$$

To calculate the doping density in our case we will be using the above-mentioned approach. With an approximate idea of the doping

concentration the extent of hole localization can also be found out.

BAND GAP VARIATION (HIGH DOPING LEVEL)

(FOR QUANTUM WELLS)

:

For low doping levels we assume the following:

1. The band structure of the host crystal is not perturbed and the band states are assumed s till as parabolic states.
2.The dopants are assumed to be independent of each other and their potential is still assumed to be the simple columbic potential.

These assumptions become invalid when the doping levels become higher. the Bohr radius of impurity is of the order of 100A. Thus after this level other impurities. At high doping levels we start getting impurity bands influence the potential seen by the impurity electron.

The following effects are associated with heavy doping levels:

1. Screening of the impurity potential: the background mobile electron density increases. This background impurity adjusts itself in response to the impurity potential. This causes the donor level to move towards the conduction band edge.
2. The electron interaction: the high density of electrons interacts with each other. This results in a downward shift of the conduction band level decreasing the energy band gap. The wave functions of electrons start overlapping each other and Pauli's exclusion principle applies. the Electrons spread their momentum in such a way that their wave functions do not overlap. The interaction is expressed in the form of coulombic and exchange interaction.

   The band gap shrinkage in any doped semiconductor can be found by:

$$\frac{Eg}{R} = \frac{1.83}{r_s}\frac{\Lambda}{N_b^{1/3}} + \frac{0.95}{r_s^{3/4}} + \frac{\pi}{2}\frac{1}{r_s^{3/4}N_b}\left(1 + \frac{m_{\min}^*}{m_{maj}^*}\right)$$

R is the Rydberg constant for carrier bound to a dopant atom and R_s is the average distance between majority carriers, normalized to effective Bohr radius.

R_s=ra/a

Where rs=(3/4πN)1/3

A=4π∈ $\hbar^2 / m^* e^2$ $\hbar^2 / m^* e^2$

Λ is the correlation coefficient for anisotropy in n- type semiconductors and for interaction between HH and LH in p type semiconductors b is the number of equivalent band extremes m_{min} and m_{max} are the DOS effective masses. The first term here corresponds to the exchange energy of the majority carriers. The second term for correlation energy and the third one for impurity interaction.

For the GaAs the band gap shrinkage is given by [5]

$$\Delta E_g = A \times N^{1/3} + B \times N^{1/4} + C \times N^{1/2} \quad meV$$

	A × 10^{-9}	B×10-7	C×10-12
p-GaAs	9.83	3.9	3.9
n-Gaas	16.5	2.39	91.4
p-AlAs	10.6	5.47	3.01

.

*the values for Al_xGa_{1-x} As are obtained by interpolation

The expression stated above takes into account exchange energy , the correlation energy and the impurity interaction energy.

Above Mott critical density the electrons in the conduction band are

assumed to exist in the form of electron gas. The band gap narrowing is very sensitive to the arrangement of donors and acceptors in the structure. Work has been done for the BGN narrowing due to different factors [6].

The point to be noticed above is that the BGN from donor electron interaction is lesser as compared to that due to others.

3. Band tailing: The formation of band tails in heavily doped semiconductors has been a subject of great study. Part of more gradual decrease of the densities of states at the band edges in heavily doped materials is attributed to fluctuations of the impurity potential, which is related to the fluctuations in the impurity density.

The band tailing in the case of QW structures has a different way of analysis.

If we start from thick layers (large *d*) and let the *d* become smaller we find that the sub bands are formed in the GaAs well. The bottom of the lowest sub band moves towards higher energy, as *d* tends to zero. A similar trend is observed for band tails.

It is clear that in case of thick layers bulk behavior is approached and in the case of thin layers the behavior of $Al_xGa_{1-x}As$ barriers is approached. For very thin layers the $\rho_{\text{f becomes}}$ very similar as that of barriers with the same average composition.

The most studied disordered systems are doped semiconductors (DSC's). The disorder here arises as a result of random position of impurities (donors or acceptors).the conduction band (valence band) edge starts penetrating in the form of a tail in the forbidden

Energy band gap as the impurity concentration is increased as the concentration is lowered an erosion appears between the body and the main tail of the band. This erosion finally becomes pronounced and leads to the formation of a separate impurity band.

At higher concentration the CB shows a tail extending towards lower energies. A concavity change in the DOS appears with the beginning of the band tail as N_d decreases the latter shrinks and the concavity change leads finally to the formation of an impurity band (IB) split off from the conduction band by an energy gap. This occurs at $N_d \sim 0.1$ (i.e. $N_d^{1/3}$ a $_0$ ~0.12 in usual units).the gap widens out as N_d decreases and tends towards hydrogenic limit(1R).at very low concentrations the CB DOS is found to be practically equal to that of free electron gas ($\sqrt{E} / 2\pi^2$) as expected . The main features of IB are; (i) its DOS is asymmetric. it falls off on its higher energy side while falls off slowly from its lower energy side and vanishes at definite energy.

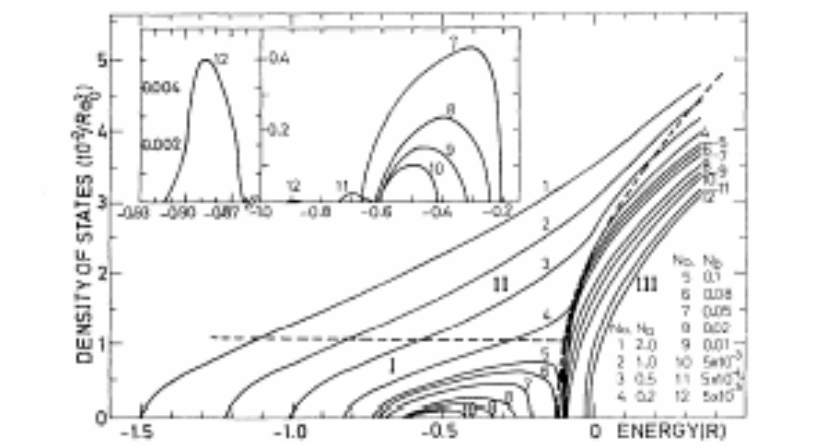

FIG. 1. DOS's as functions of energy for different impurity concentrations N_D. The insets show the impurity-band DOS's (enlarged scales) for several concentrations. Regions I, II, and III delimited by dashed lines are domains of existence of localized, hybrid, and extended states, respectively (see Sec. VI).

For all explored concentrations the integrand DOS over the IB when it exists is equal (to within a few %) to the impurity concentrations as it should be. According to the Sum rule the states Formed in the IB are all derived form the main band such that the total number of sates are invariant. The results obtained by scattering at all impurity potentials and those obtained in the higher density approximations differ only in the lower energy range

(concavity) confirming that the multiple scattering effects at higher energy range are negligible. In the lower energy region the scattering method leads to a more extended tail into the band gap.
If one assumes the activation energy to be close to the energy gap between IB and CB, the critical concentrations which corresponds in our calculations to the closing of the energy band gap ($N_d^{1/3} a_0 = 0.12$) is about 10 times smaller than the experimentally observed one. This discrepancy ought to be ascribed to the lack of multiple occupancy corrections. This is likely to be due to the use of TF potential, which is over screened at this impurity concentrations and deviates markedly from the true potentials. To verify the assertion the above calculation had been made by enhancing the impurity potential by multiplying it with a constant and alternatively increasing the screening length.

As mentioned before there always exists certain amount of BGN in semiconductors this shrinkage arises from the VB and the CB shifts inside the band gap due to exchange correlations and the electron impurity interaction term. The ends of the tail (above Mott critical density) decide the energy band gap. But the important point that comes into picture is the density of states that are available. It should be noted that the two interactions described above are more strong in the VB than that in the CB .due to this though the CB tail is more extended in the BG but the density of states of VB is twice as that of the CB. It is important to note that while observing the optical properties the band gap shrinkage is partly compensated by Bur stein Moss Shift.(or Phase space filling in heterostructures). As seen above the absorption wavelength is lower than the expected transition wavelength. This is known as Phase Space Filling described in the other sections.[1,2].

Binding energy of donors, acceptors, donor bound complexes in quantum wells:

Binding energy of the acceptors in QW:

I will be using the binding energies calculated by W.T.Masselink (1983) which has been calculated for infinite well which quite well applies for our case since the well width is high.(mistake might be only due to degeneracy of light and heavy holes in QW).although the holes spatial confinement due to QW lifts the holes degeneracy the impurity potential will still be sufficiently deep to significantly couple the HH and the LH bands. The case is not same as that of an exciton where bands are completely decoupled. The variation of the binding energy with the well width is given in the figure. As the well width approaches zero the binding energy becomes equal to that of that n AlGaAs barrier. Increasing the well width from zero, the symmetry is decreased and this single level splits into two levels (HH and LH respectively). The energy due to LH is greater than HH for well width greater than 40 Å For well width greater than 200 Å the binding energy for the two levels is essentially the acceptor BE (in bulk) plus the HH and LH sub band energy measured from valence band edge. The binding energy for carbon as an acceptor corresponds to 28 meV for our case.

Binding energy of the donors in the quantm wells:

The energy variations are very much similar to that of acceptors. As the well size decreases an increase in the barrier thickness from zero tends to more strongly localize the wave function around the impurity ion and thereby increasing the binding energy but for a finite barrier height V_0, increase in the barrier thickness from zero adds a repulsive term in the energy due to wave function penetration in the barrier thus reducing the binding energy [4].

In the case of GaAs wells in the binding energies of Si (as in our case) is very small as compared to the acceptors

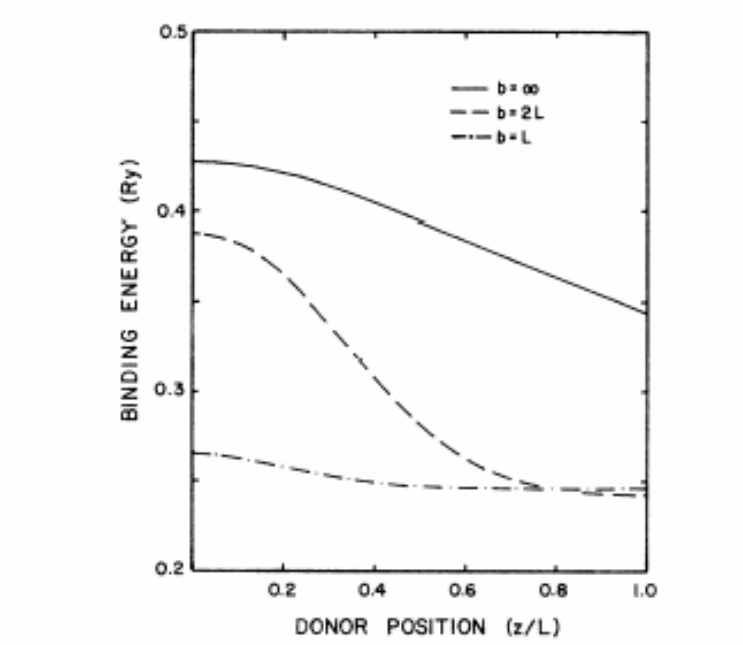

FIG. 2. Binding energy of the lowest $m = \pm 1$ excited states of a shallow donor in a $Ga_{1-x}Al_xAs$ well as a function of donor position. The aluminum fraction is $x = 0.3$ and $L = 1.0a_0^*$.

Binding energy of the D^0X complex

Haynes as gave an empirical relation between the binding energy of the complex and the donor binding energy:

$$E_1 = BE_D$$

Where B is the proportionality constant dependent on the impurity

(for Si, B = 0.1)

According to the study of Reynolds the donor binding energy as a function of the well width and the HHFE is as it is plotted as in the figure.

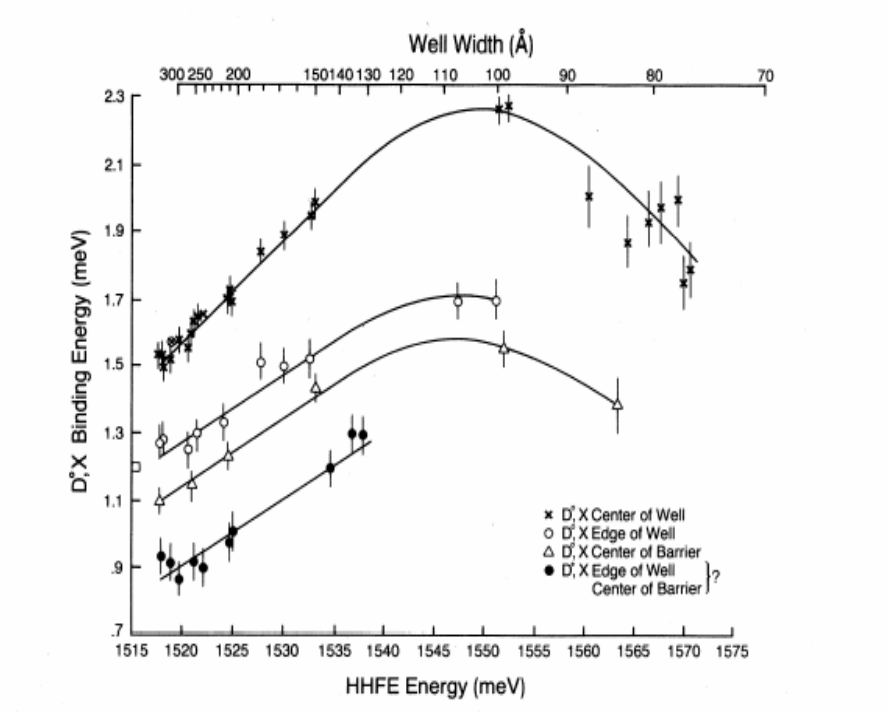

Figure - variation of the D^0X transition with well width

The binding energy is different for the position of the donor across the well i.e. center of the well, edge of the well and the center of the barrier.. The binding energy of the complex increases for all three cases as the well width is reduced for all the three doping. Situations. However for the well width of about 100 angstrom they tend to reach their respective maximum values.

The figure on pg 24 plots the variation of the binding energy of the D^0X complex with well width (for a case similar to ours).

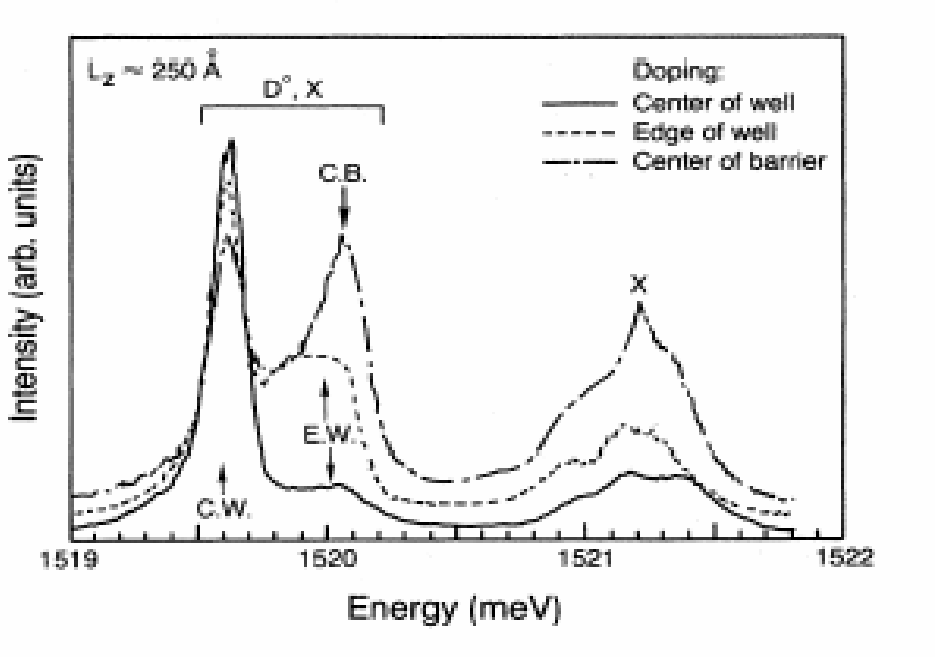

Figure - variation of D^0X transition energy in 250Å quantum well

Experimental:

The uniformly doped GaAs/$Al_xGa_{1-x}As$ MQW structures studied here were grown by Metal organic vapor deposition method (MOCVD) on an n^+ semi insulating GaAs substrates. The growth sequence consisted of Germanium substrate followed by GaAs buffer layer, followed by MQW's. The MQW's consisted of 28 periods with a barrier width (L_b) of 300 Angstrom and a well width of 300 Angstrom(the well width will accurately be determined by PL with the help of peak energy).The well was uniformly doped with Si do pant with a concentration of $2x10^{18}$ as

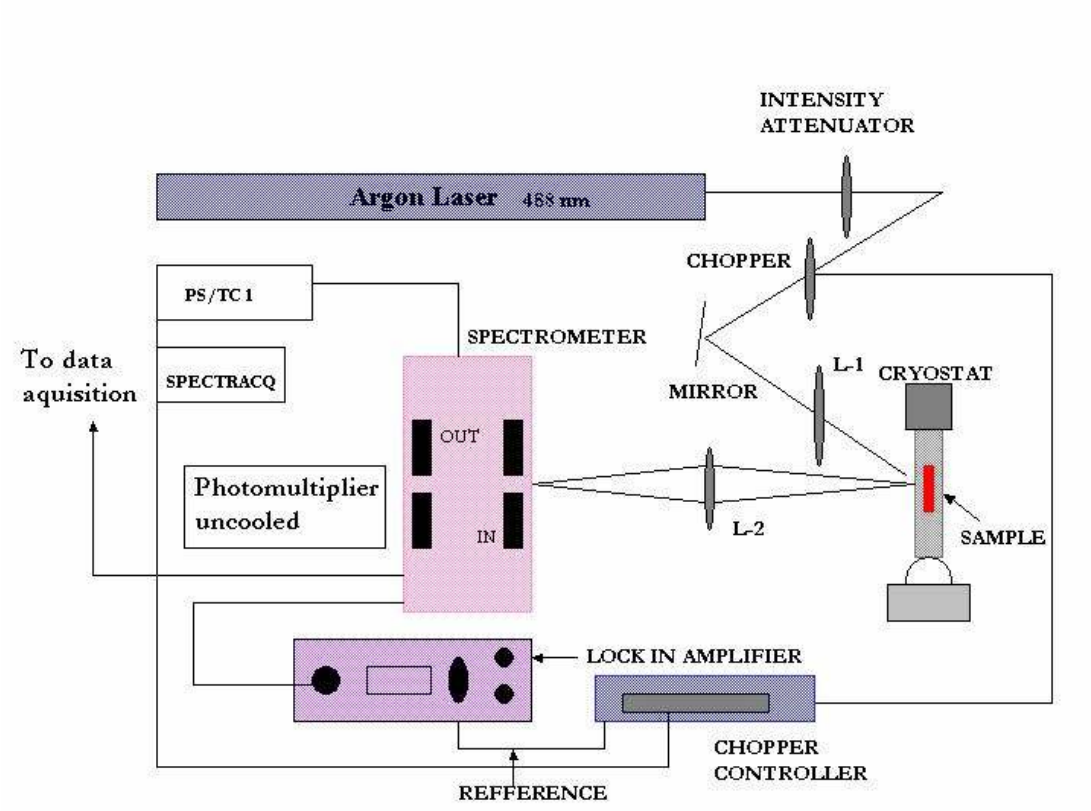

given by ECV measurements. The barrier is unintentionally doped with a concentration of $1x10^{13}$. The corresponding carrier concentration in the well at low temperature due to barrier will be found out using PL technique). Figure shows the structure used and the energy band diagram of the well had the well been undoped (modulation doping).

Experimental setup:

A variable intensity but almost fixed wavelength (450nm – 500nm) Argon Laser was used for photoluminescence measurements. Lens 1 was used to concentrate the light on the sample and an optical chopper was used in conjugation with a lock in amplifier to filter out the noise and recover the weakest signal buried in the noise. the use of optical choppers ensures that only the light emitted form the sample is being detected. the optical beam thus chopped by the row of slots is used as a reference for the lock in amplifier.

The sample was placed in a Liquid Helium cryostat .the temperature is reduced to control the thermally excited recombination processes and obtain fullest spectroscopic information. an important fact of the system was that we needed a vacuum better than 10-3 mbar to isolate the cold parts of the system from the surroundings. the vacuum acting as a thermal insulator prevents condensation of water vapor on the surface of the system .therefore we had a rotary pump which could provide a pressure of 5 times 10-4 mbar(see cryostat details).

Lens 2 was used to collect the light from the sample. the light was detected using TRIAX 320 spectrometer .this had a Ge detector(see spectrometer details).the light is measured by Photo multiplier (PM) and the signal coming out of the PM could be amplified .Spectral data were recorded with help of a spectrAcq2 and SpectraMax software.

The spectrometer

Focal length	**320 nm**
Spectral range	**0 – 1500 nm range mechanical range (1200 g/mm grating)**
Aperture	**F/4.1**
Dispersion	**2.64 nm/mm**
Resolution	**.06 nm (single slit)**
Accuracy	**+/- .03nm**
Repeatability	**+/- .06 nm**

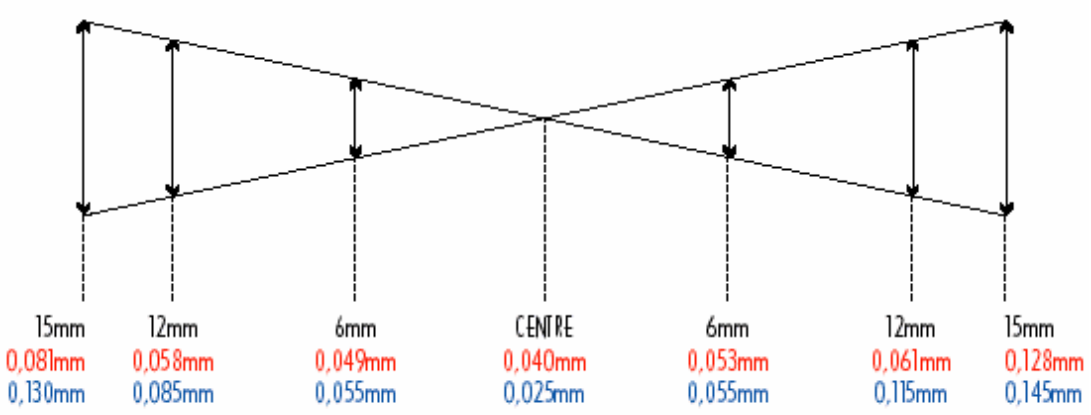

Figure: IMAGING PROCEURE

The incident light passes through the entrance slit and hits a collimating mirror that produces a parallel polychromatic light beam onto a diffraction grating. The grating spatially separates the spectrum of the incident light and the focusing mirror reflects the diffracted light onto the exit slit. Each wavelength is incident upon exit plane at a specific angle. Rotating the grating position scans the wavelengths across the exit slits discriminates between each wavelength.

The grating angle specifies the angle that is required to bring each wavelength on the exit slit.

The slits play an important role in determining the resolution, throughput and the quality of spectrum through a spectrograph. In most cases they are adjustable and can vary from a few microns to a few mms

Metal Organic Chemical Vapor Deposition (MOCVD)

The samples were grown in our laboratory the MOCVD growth technique. This technique produces heterostructures of very high quality. The apparatus usually operates at atmospheric pressure. The substrate sits on a heated block in a chamber through which different gases are passed in a carrier of hydrogen; the composition of the gases can be varied rapidly to control the composition of the material grown. The basic reaction for deposition of GaAs is between a metal alkyl and a hydride of the group V material and is given by :

$$(CH_3)_3Ga + AsH_3 \rightarrow GaAs \downarrow + 3CH_3 \quad (650°C)$$

Depending on the temperature, growth may be limited by the rate of reactants diffuse through this boundary layer or by the rate at which the reactants reacts at the surface. The volume of the sample between the mixing of the gases and the substrate must be minimized to change the composition of the gas and the resulting semiconductor rapidly and give sharp interfaces.

Device processing and its importance in the PL study

It is obvious that PL study does not need any sort of formal sample preparation (Because the surface layer has to undergo the study). But since the devices, those are to be characterized consist of several different epitaxial layers, we need to carry out some device processing steps (Basically etching) prior to the PL experiment. So it is good to describe the device processing steps in the report.

The devices grown by MOCVD reactor At MRC, IISC, Bangalore consists of different combination and composition of GaAs/AlGaAs epitaxial layers for optoelectronic device applications. The AlGaAs layers are never kept at the top surface as they are very sensitive to earth's atmosphere. So to Pl characterization of the layer one has to etch the GaAs layers and has to stop exactly at the AlGaAs layer just before the experiment. So for this particular study, wet chemical etching method was employed to etch the top highly doped GaAs surface by using citric acid: hydrogen peroxide and water based selective enchant. Since the thickness of the top layer was confirmed by ECV profile and the etch rate was standardized in our lab, hence the top layer was etched upto the exact depth. Then the sample was loaded for the AlGaAs layer PL study.

But for the case of GaAs/AlGaAs quantum well structures the sulphuric acid: hydrogen peroxide and water based wet chemicals are used to get the proper epitaxial layer to be exposed to the incident LASER light in the PL set-up. Though the device processing techniques appear to be simple, it is not so, because it needs the exact precession on the temperature, humidity and time control (Since the layers we are dealing with are of Angstrom level thickness). So it was possible because of the class 100 clean room facilities available at MRC, IISc, Bangalore.

Introduction to heterostructures and the calculations of energy states QUANTUM WELLS.

The properties of the bulk materials are no longer valid in the case of

nanostructures when the mean free path of an electron becomes greater than the geometrical dimensions of the structures. Real electrons are 3D but can be made to move in fewer dimensions. Trapping the electron in the narrow potential well where the motion can be only along two dimensions can do this. And the electron tends to remain confined there. In such a potential well, the energy of the states is quantified along the direction perpendicular to the *z*-direction.

The wells in the QW structures are practically isolated. The lowest energy level of the conduction band lies above the minima in the conduction band..

The depth for electrons is set by the discontinuity in the conduction band ΔE_c that is usually kept below 0.3 meV to avoid indirect band gap in AlGaAs. The discontinuity in the valence band is even smaller 15% of ΔE_g. The size of the conduction band discontinuity plays an important role in calculations. Duggan [15] made a lot of measurements of the PLE spectra and gave the ratio as 65:33, which is now well accepted.

The well depth is given by ΔE_g or V_0 .the potential should be curved rather than the straight one used here. This is done to make the comparisons with an infinitely deep well simpler.

Calculations of the energy states in a potential well with finite barriers: Schrödinger equation:

$$\left[-\frac{\hbar^2}{2m}\nabla + V(x)\right]\psi(x) = E\psi(x)$$

with $-\frac{\hbar^2 k_E^2}{2m} = E$ (D1) $-\frac{\hbar^2 k_E^2}{2m} = V_0$ (D2) $-\frac{\hbar^2 k_E^2}{2m} = E - V_0$ (D3)].

Equations for area I, II and III are:

(i) $$\left[-\frac{\hbar^2 d^2}{2m dx^2} \right] \psi_I(x) = \left[-\frac{\hbar^2}{2m} k_E^2 \right] \psi_I(x)$$

$$\Rightarrow \quad \left[\frac{d^2}{dx^2} - k_E^2 \right] \psi_I(x) = 0$$

(ii) $$\left[\frac{d^2}{dx^2} + k_{E-V}^2 \right] \psi_{II}(x) = 0$$

(iii) $$\left[\frac{d^2}{dx^2} - k_E^2 \right] \psi_{III}(x) = 0 \quad .$$

Confined states are only possible in (ii).

The fundamental solutions are:

$$\psi_I(x) = A_I e^{k_E x} + B_I e^{-k_E x}$$

$$\psi_{II}(x) = A_{II} e^{ik_{E-V} x} + B_{II} e^{-ik_{E-V} x}$$

$$\psi_{III}(x) = A_{III}e^{k_E x} + B_{III}e^{-k_E x}$$

Since $(\psi \xrightarrow{x\to\pm\infty} 0)\ B_I = A_{III} = 0$.

Solving the three transcendental equations and using D1 leads to the energy eigenstates of the potential barriers of finite height.
If the potential barriers are of infinite height V_0 is - ∞ and so $k_{\text{E-V}}$ becomes + ∞. This leads to

$$k_{E-V}a = \frac{\pi n}{2} \qquad \text{Where n = 1,2,3,4,…..}$$

and with E=E-V_0 to the eigen states :

$$E_n^* = \frac{\hbar^2}{2m}\left(\frac{n\pi}{2a}\right)^2$$

(figure attached in the next page)

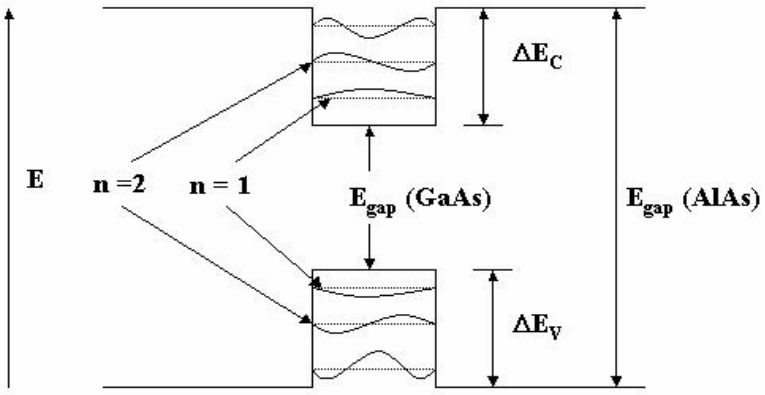

ANALYSIS AND DISCUSSION:

The structure here used was unetched solar cell. The PL spectra were taken in presence of the highly doped p+ GaAs (10^{20} doping of Zn) layer on the top surface. The structure is as given below:

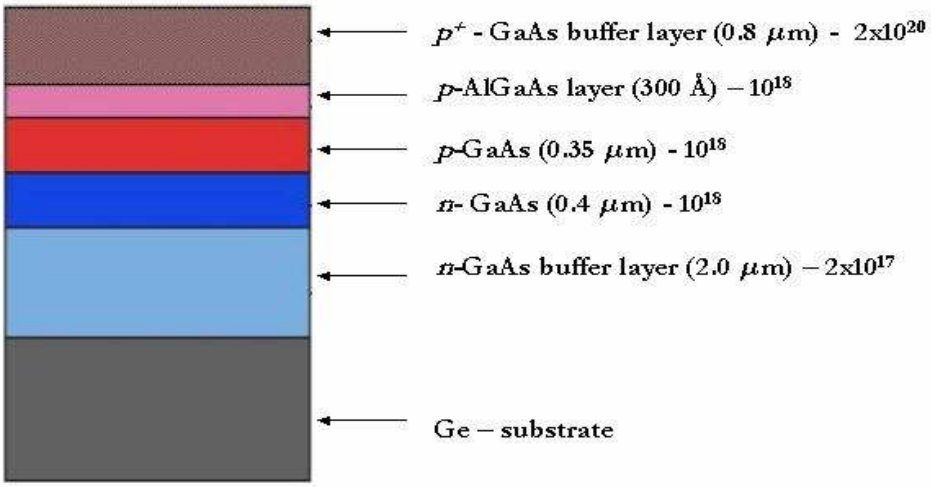

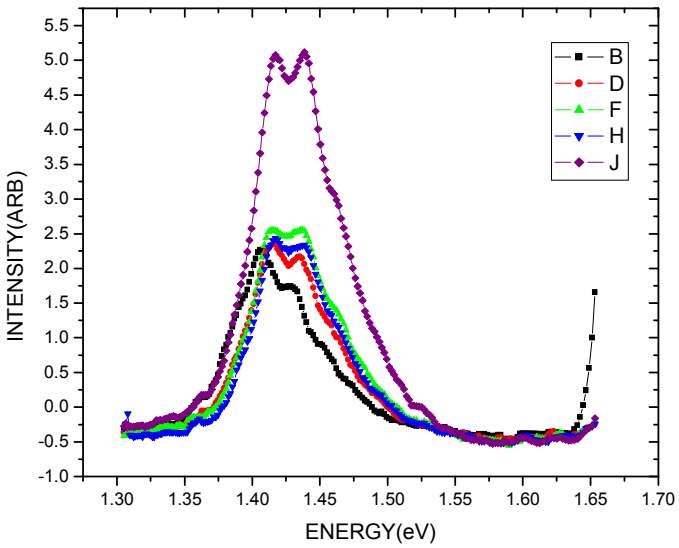

A double peak that is seen here. Comparison of the two spectra's shows that the high-energy anomalous peak at high temperatures that

was observed earlier is no longer to be seen. That means the peak was associated with the third layer and could be because of the type-II transitions that take place at the interface. Since the transmitted light is of very low intensity after the presence of the p^+ - GaAs layer that is now present.

There are two peaks that are visible .the second peak is a shoulder at high temperature but its intensity becomes comparable to that of the first at low temperatures indicating the saturation of the intensity of the first peak.

The comparison of the second peak for temperature variation with earlier studies [17] shows that the second peak is attributed to the e-A transition because the impurities are not fully ionized at lower temperatures. The recombination of the electrons in the conduction band via acceptor and valence band are possible at low or medium doping levels. At higher doping levels the impurity wave functions overlap and impurity bands are formed. Thus as acceptor

concentrations increase the activation energy reduces to zero($p > 1.4\times10^{19}$)in this situation miller[19] suggested that transitions via impurity level may not occur. So the main peak was due to B-B transition and not e-A but Nasledov suggested that e-A transitions are possible even for heavy doping levels. Here we conclude that the transitions are e-A type. The intensity of the transition increased as the temperature decreased (or concentration increased),the intensity of BB transition is too weak to be observed at high doping levels. Hence dominant transition at low temperatures is e-A transition.

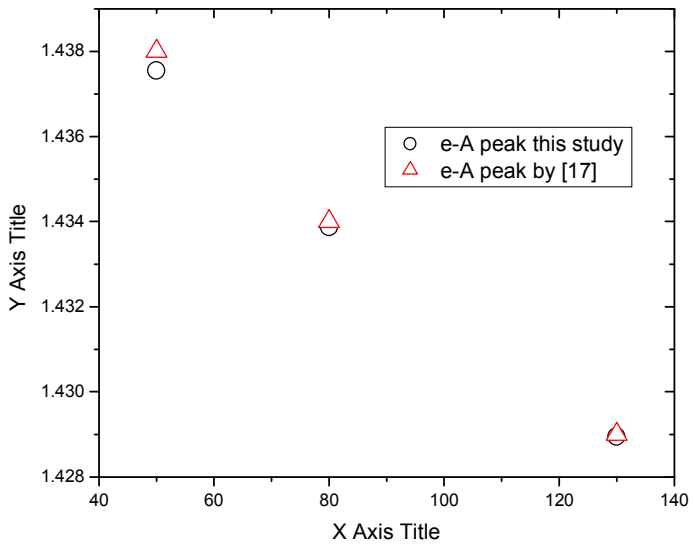

Comparison of the e-A transition energy of [17] and our study

the shoulder that constantly appears in the spectra and shifts to higher energy with decrease in energy is next to being analyzed. The intensity of the peak increases with the same proportion as that of the main peak. The peak also exhibits homogenous broadening at higher temperatures. Now there is a shoulder at around 1.46 i.e. lower than the energy of main shoulder. Had the transition been attributed to the band bending of the next layer it would have been on a much higher side of this peak (since the next layer is that of AlGaAs) hence this could be attributed to the K non conserving (indirect or non-vertical transitions) optical transitions. The transitions were found to be on the higher energy side with increasing concentrations. The transitions were known to be between the conduction band and the Fermi energy level below the top of the valence band. Therefore PL spectra were found to be a combination of both indirect and direct transitions. The shoulder was found to shift at higher energies with increasing temperatures.

The high energy shoulder that appears in the spectra below

temperatures 50k and becomes more obvious as the temperature is decreased or the concentrations is increased [17],[18].the shoulder peak is positioned around 1.52±.007 eV. This peak could be attributed to the luminescence associated with the depletion layer. The depletion layer is due to band bending between the AlGaAs layer and the heavily doped GaAs top layer. The excitonic peaks appear to dissociate at higher doping concentrations due to low binding energies. Hence the peaks cannot be attributed to excitonic transitions.

The low energy peak can be explained as being a part of the band to acceptor transition [17].as the hole concentration increase the impurity band moved towards both the valence band and the forbidden band for further increase in the hole concentration. The spread of the impurity band towards the forbidden gap was faster than n the valence band edge. There are many states in which the conduction band electrons in the impurity band may recombine. These states may be the interaction of the defect type acceptors (ZnGa or CGa) and the normal acceptors. The highest density of hole states in a heavily doped semiconductor lies at the top of the impurity band.

The temperature variation of the intensity is given below. It could be explained by localization of the holes in the intermediate impurity levels with temperature decrease.

This PL spectrum was primarily taken out to inspect the transitions in AlGaAs structure, for this reason the layer f GaAs was etched before PL measurements.

The PL emission spectra at various temperatures were first investigated. The PL line shapes became sharper and shifted to higher energy as temperature had increased. One very odd feature that has been found to be shown by it is the peak at 300k. it is seen that the peak is at a different position as expected . This gives us an idea that the peak is of different origin than the ones found at lower

temperatures.

The main peak shifted towards higher energy can be explained by the increase of band gap of the material. This could be explained by electron-phonon interaction. Lego and Cardona [16] have shown that the Varshini's equation is valid for heavily doped semiconductors as well.

And can explain the shift towards higher energies of the main peak.

It has been shown [17],[18] that the PL spectra of Zn doped samples always shows up a shoulder 'S' at the higher energy side of the PL spectra. This is not found in our spectra indicating the concentration range. From the graph given below we can easily observe that the shoulder is not present for concentration near about 3×10^{18}. That verifies the carrier concentrations measured by other techniques. The main peak here is attributed to the (e,A)free to bond transitions .at 20k the studies[17],[18] show that the main peak is at about 1.48eV but our peak is shifted to slightly higher energy . this could be explained by the filling of conduction band (Burstein Moss shift[19]) due to photo excited electrons that travel across the junction from AlGaAs to the GaAs layer. The FWHM that comes to be around 10meV [17] is also broadened here 17meV due to the contribution in carrier density due to the AlGaAs

The peak energies for our case and the energy band gap are plotted in

the given figure. The point at 23k shows the peak energy that is in absence of AlGaAs layer. The difference between the band gap and the peak energy is due to the binding energy of the acceptor but that difference does not correspond to the binding energy of the acceptor due to filling of conduction band. As the temperature increases the difference between the energy band gap and the peak energy becomes smaller indicating that band to band transitions occur at higher temperatures (the range due to the band tailing that is there.)This also indicates the decrease in the filing of conduction band in the GaAs layers due to the AlGaAs layers.

The anomalous nature of the peak at higher temperatures has not been explained. Some studies show that the peak is related to the type-II transition at the heterojunction. Due to poor quality of the interface (not sharp). Some show that these are associated with deep level traps formed by acceptors and donors in the AlGaAs structure. Some also show that this may be due to band bending between heavily doped AlgaAs and the GaAs layers.

The FWHM shows the trend of inhomogeneous broadening with temperature. Secondly the broadening is within very narrow limits .the variation can be seen to be within 5 meV. Whereas the disagreement between the peak energy without the AlGaAs layer and with it is of the order of 20 meV (graph). This shows that the effect of phase space filling dominates all the other effects.

No.	temperature	FWHM	**No.**	temperature	FWHM
1.	10	25.7	4.	124	30.2
2.	23	25.8	5.	170	30.8
3.	74	29.1			

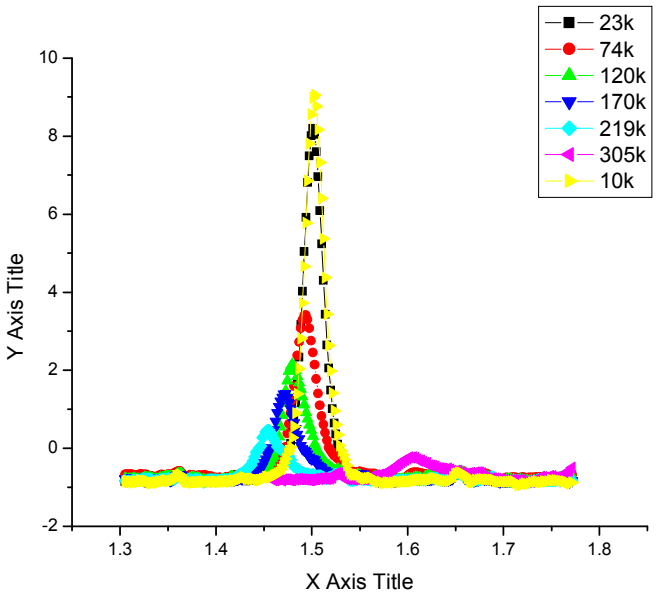

figure: the photoluminescence spectra of solar cell

QWIPS

Here we start the analysis of the QWIPS structure that has been etched from the top layer.hence the part exposed is only that of the QW . the quanrtum well that we have. The quantum wells that we have used are doped with the following concentration.we already know that the QWIPS structure consists of bound staes in between the two band edges for GaAs and AlGaAs layers.

Now the energy of bound states that we have used are corresponding to the square wells with finite barriers:

$$E_v(0) - E_v(n) = \frac{\hbar^2 \pi^2 n^2}{m^* m_h a^2}$$

$$E_C(n) - E_C(0) = \frac{\hbar^2 \pi^2 n^2}{m^* m_e a^2}$$

where $E_c(n)$ is the energy of the n^{th} bound state

The value of the effective maass and other parameters has been extracted from the bibliography of Adachi on GaAs materialson the basis of a few valid assumptions.the effective mass that is of our use is close to that of bulk GaAs and hence the corresponding variations can also be used .in our case the temperature variation is not that huge that we take the variation of masses. to take into account the carrier concentration the value of effective masses has been increased by .005(for electron).

$M_e = 0.067$

$M_{hh} = 0.34$

$M_{lh} = 0.094$

Second consideration is the energy band gap variation. the energy corresponding to the intrinsic GaAs is equal to 1.5115 at this temperature using Varshini's equation with parameters as stated before.

For the QW structures it has been shown that the different transition energies can be fitted well with the varshini's parameters as:

$$\beta = 204$$
$$\alpha = \left(5.4 \pm \pm 0.2\right) \times 10^{-4}$$

But here we will concentrate our analysis to a temperature of 11K extending the interpretation to different temperatures.

A band gap narrowing of 115.45meV is being calculated as per the equation stated earlier. Now the filling of lower energy compensates the optical transition band due to higher carrier concentration. Second point

to be noted is the phase space filling (section) and its effect on the spectra.

1.39605 eV gives the band gap as calculated due to BGN. The intrinsic energy band gap is 1.522. the higher energy transitions are because of the presence of the bound states.

Now it has been shown that [13] the dominant transition in n - type wells is due to D^0X transitions that take place. The binding energy of this corresponds to some 9 meV in case of low doping levels. The binding energy is expected to decrease slightly in our case due to the effect of carriers contributed from the barriers. Also it has been shown that the excitonic binding energy only is affected in the filled sub band. the other sub bands excitons are not affected by it.

It has been shown that in case of n type GaAs the peak energy corresponds to the value of about 1.523eV and the energy band gap is 1.46837 at the carrier concentration of 1018. The Burstein-Moss shift is of about 7 meV (since ΔE_g is 50.37 meV). Hence the energy increase due to the bound states must be of the

Order of the difference in the peak energies. But one more point here to be considered is that the binding energy here increases greatly. Hence the shifts expected will more than the actual value.

After calculations, the well width here is been established as being about 250Å. The energies of the corresponding bands (for n^{th} sub band) is given as:

The energies of

CB: $13.104\ n^2$ meV

HH: $2.56176n^2$

LH: $0.\ 26813n^2$

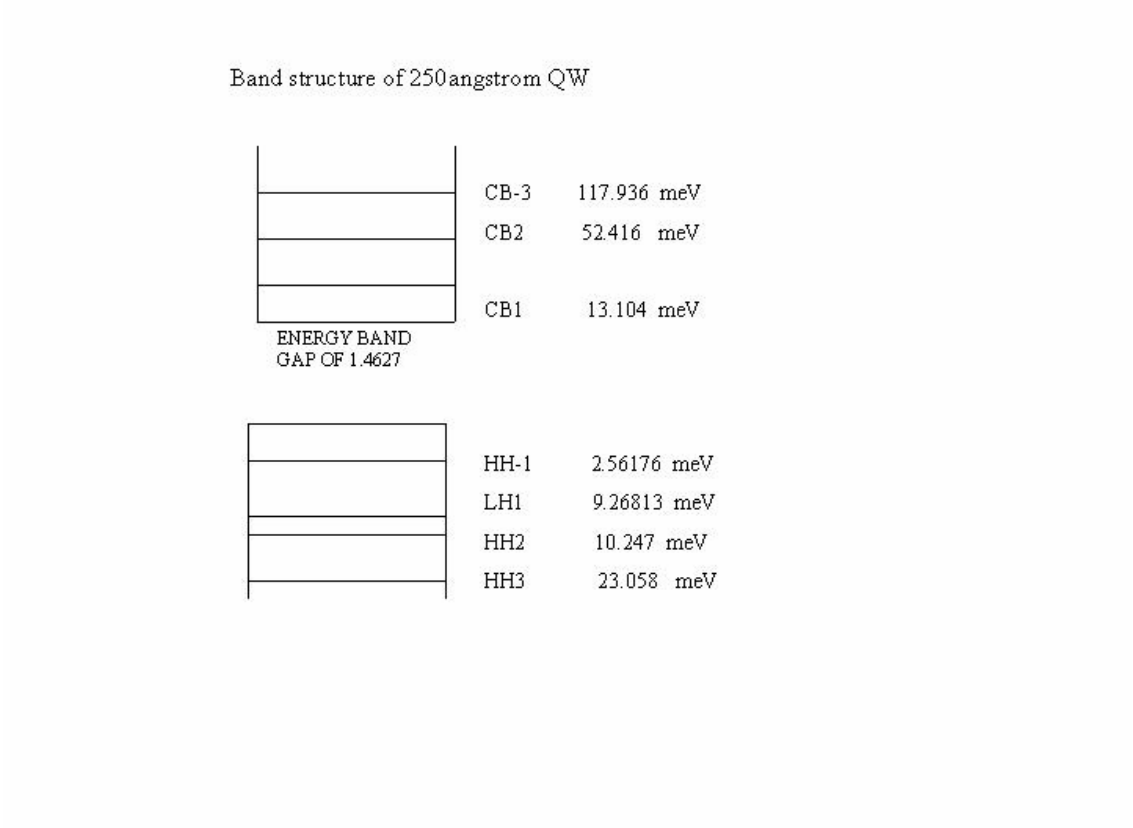

Figure – Bound States in 250 Å Quantum Well

From the earlier analysis of the quenching of the excitonic for modulation doped heterostructures has been shown that the excitonic peak (n=1) quench at a carrier concentration of about 1011 and that the HH and the LH peak merge and are almost bleached out. The peak energy at 1.4 78 is attributed to n=1 HHX-D and LHX-D transitions. The many body effects are important in this case. The study of the energy variation with intensity of excitation shows that the peak gets saturated with increasing intensity. Also the peak was not found at higher temperatures. This could be explained by the filling of the CB-1 level and quenching of the peak. As

the temperature is decreased the number of ionized donors decrease and extrinsic carrier concentration decreases. Also the linewidth of the peak was narrowed as the intensity of the excitation was increased. This indicates that the empty states in the band decrease and finally with the highest intensity the empty states are not left. The increase in the carrier concentration with increasing energy does not shift much the CB1-HH1 energy due to the reason that [1] the band gap renormalization decreased the band gap by the same order as the decrease in binding energy of the exciton as due to screening. The quenching of the excitonic peaks is at approximately concentration of 1011. Hence the carrier concentration due to the donors and the edge of the barrier dopant is approximately given by the 1011.the FWHM of the HHFX-D transition is plotted as a function of excitation intensity indicating the filing of the band states. Since the peak is attributed only to the excitonic transitions (readings taken at low temperature) the FWHM of the graph gives us an idea of the excitonic lifetime by

s.no.	FWHM	Lifetime (in ps)
1	0.024	0.00625
2	0.04	0.005
3	0.067	0.8

Earlier measurements of the CB-HH transition have been listed in table. Now the linewidth in our results corresponds to the carrier concentration

of 10^{11}.

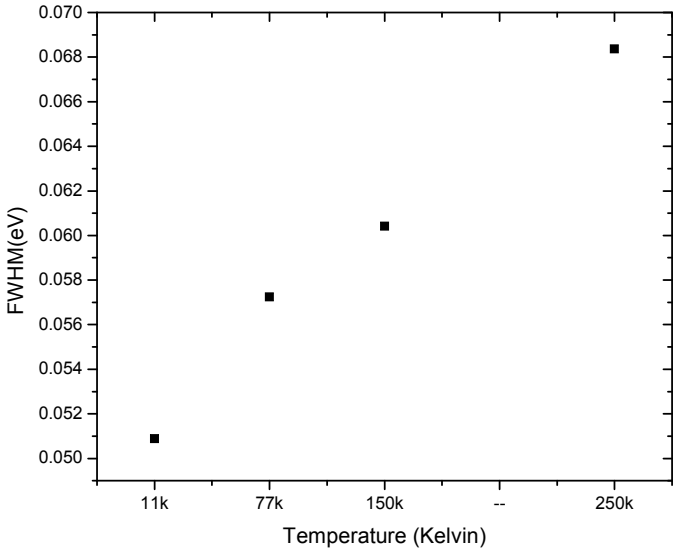

Doping	*FWHM*
$0.2x10^{10}$	6
$1x10^{11}$	10
10^{12}	12
10^{11}	21

FWHM variation by[1]

The first peak energy increases greatly as the temperature increases and the intensity does not saturate even at higher temperatures.

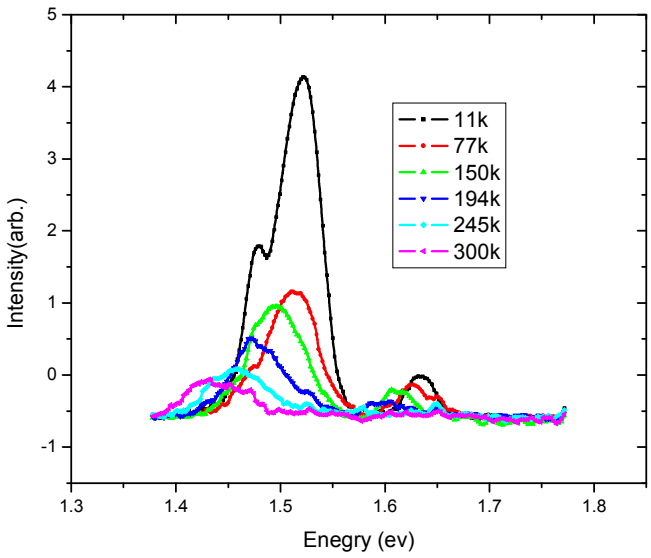

Figure – PL spectra of 250 Å Quantum Well at different temperatures

The second peak at 1.5215 corresponds to the HHX-D^0X transition. The peak shows similar nature as that of the first peak with the only difference that the peak does not saturate at higher energies. This is because of the available density of states at n = 2

level.

The behavior of the third peak is very much similar to that of the other two. Hence it could be attributed to the HHX-D (n = 3) transition. But the disagreement between the calculated value and the observed value is high in this case. This could be explained by the non- validity of the parabolic bands and the hole effective masses. Introducing AlGaAs lateral barriers does not modify the PL spectra significantly. If AlAs barriers are grown at both the sides of the GaAs QW the CB1 – HH1 peak broadens. This may be due to impurities at the interface or due to variations in the thickness of the layers.